Journal of Materials Chemistry C

Accepted Manuscript

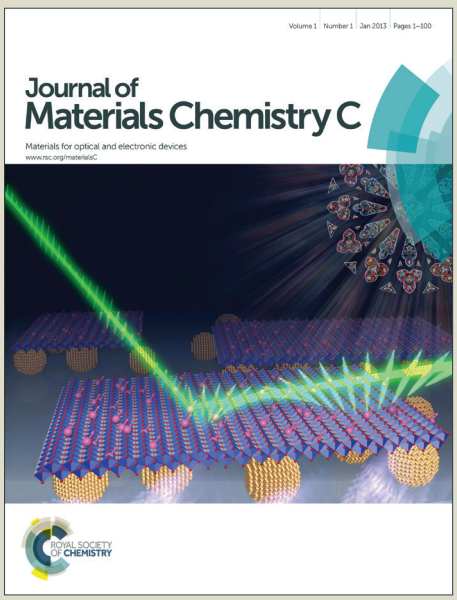

ROYAL SOCIETY OF CHEMISTRY

www.rsc.org/materialsC

Optimized photoluminescence of red phosphor $K_2TiF_6:Mn^{4+}$ synthesized at room temperature and its formation mechanism

Lifen Lv,[a] Zhen Chen,[a] Guokui Liu,[b] Shaoming Huang,[a] and Yuexiao Pan[a*]

[a]*Nanomaterials and Chemistry Key Laboratory, Faculty of Chemistry and Materials Engineering, Wenzhou University, Zhejiang Province, Wenzhou 325027, P. R. China. Tel. & Fax: (+86) 577-8837-3017. E-mail:yxpan8@gmail.com*

[b]*Chemical Sciences and Engineering Division, Argonne National Laboratory, Argonne, IL 60439, USA.*

†Electronic Supplementary Information (ESI): photographs of the phosphor samples under visible and UV lights; XPS of KTFM; characterization of the sample prepared from TiO_2 as a titanium source; the structure projection of KTF; comparison of emission spectra of samples prepared from different titanium sources; XRD patterns and decay curves of samples obtained at different $KMnO_4$ concentrations; the influences of HF concentration on excitation spectra, decay time, luminescence intensity, and yield; thermal stability of KTFM; photographs of purple LED and "warm" white LED fabricated with $K_2TiF_6:Mn^{4+}$.

Abstract

A red phosphor $K_2TiF_6:Mn^{4+}$ (KTFM) has been synthesized by etching $Ti(OC_4H_9)_4$ in HF solution with $KMnO_4$ and KF at room temperature for 30 min. The formation mechanism of red phosphor KTFM has been discussed based on detailed experimental results. We studied the influences of synthetic procedure and $KMnO_4$ concentration on the powder color and intensity of phosphor luminescence. The actual doping concentration of Mn^{4+} in the K_2TiF_6 (KTF) host lattice of the phosphor has been investigated by measuring the concentration of filtrate through ICP-AES analysis. The results showed that about 32.4 mol% of Mn elements was doped into KTF crystals at optimal Mn^{4+} concentration (in precursor solution). The presence of HF was found to be essential to doping Mn^{4+} into KTF due to the weakly acidic and complexing properties of HF. The red luminescence of Mn^{4+} in KTF with a crystal structure matching standard card JCPDs (#28-0825), was first observed in the sample prepared from HF solution concentrations lower than 5 wt. %. The dependence of the intensity of the luminescence on HF concentration might be due to the varying of Mn^{4+} concentrations in KTF crystals. Higher HF concentration was associated with lower yield, because KTF is soluble in HF at high concentrations. Encapsulation of the red phosphor KTFM with YAG:Ce on a GaN layer produces "warm" white LEDs with color rendering of 86 at 3251 K.

Introduction

The global energy crisis has drawn considerable attention to solid-state lighting fabricated with blue GaN chip and yellow YAG:Ce phosphor, which is a low-energy, long-lasting, and environmentally friendly alternative to traditional lighting.[1-3] Poor color rendition is one of the problems with this kind of white LEDs, and is attributable to the lack of red components in luminescence of phosphor YAG:Ce. This limits their utility in lighting.[4,5] Modified garnet derivatives (such as $(YGd)_3Al_5O_{12}$:Ce) have better emission power distributions in the red region but this improvement comes at the expense of energy efficiency.[6,7]

Extensive efforts have made toward improving the color rendering index of white LEDs by developing red phosphors with excitation bands in the blue region.[8-11] Because of high quantum efficiency and strong absorption in the blue, significant research efforts have been directed toward the preparation of red phosphors of Eu^{2+} -doped nitrides. One of them is available commercially.[10,11] However, critical synthetic requirements and a scarcity of nitride phosphor starting materials makes them somewhat costly. A class of red phosphors with Mn^{4+} ions as luminescence centers are alternative candidates with simple synthetic processes and an abundance of starting materials; this is because the phosphors do not include rare earth elements.[12-24] Mn^{4+} doped alkaline aluminates showed promise in white LEDs but the efficiency of their luminescence requires further improvement.[12-14]

Red phosphors composed of Mn^{4+} doped in complex fluorides $A_2XF_6:Mn^{4+}$ (A is K or Na; X is Si, Ti, Ge, or Zr) and $BaXF_6:Mn^{4+}$ (X is Si or Ti) show a broad absorption

band that overlap the electroluminescence band of GaN chip.[15-29] Large Stokes shifts and sharp emission peak indicate that they are more suitable than Eu^{2+}-doped nitrides due to their small re-absorption when mixing with phosphor YAG:Ce. The red phosphor KTFM was obtained by immersing 1.0 g TiO_2 (or Ti metal) in 50 mL of 50 wt. % HF, 1.5 g $KMnO_4$ and 2.0 g KF. [24] However, its mechanism of formation, which is relevant to luminescence efficiency, has not yet been investigated. Considering that luminescence efficiency is strongly related to synthetic conditions, it is necessary to elucidate the formation mechanism of red phosphor KTFM and optimize its performance. Recently, an efficient cation exchange reaction has been used to synthesize red phosphor KTFM.[25] In that procedure, the reaction was completed by mixing KTF and K_2MnF_6 in HF at 70 ^oC for 3 h and the as-obtained phosphor showed luminescence quantum yield as high as 98%. K_2MnF_6 is not commercially available and its synthesis is complicated.[30]

In this paper, we obtained KTFM by etching $Ti(OC_4H_9)_4$ (or TiO_2) in solutions mixed with (5-40 wt. %) HF and (5-60 $mmol.L^{-1}$) $KMnO_4$. The concentrations of HF and $KMnO_4$ are much lower than those used in previous work (50 wt. % HF and 330 $mmol.L^{-1}$ $KMnO_4$).[24] The synthetic technique is facile and mild but the mechanisms of formation are complicated. The properties of the samples are strongly dependent on the experimental procedure and the concentrations of the starting materials. The optimization of the synthesis conditions led to improved the luminescence intensity of KTFM, which is significant for practical applications.

2. Experimental

2.1 Synthesis

All reagents were standard grade and used without further purification. The starting materials $KMnO_4$, KF, $Ti(OC_4H_9)_4$, HF and H_2O were mixed under magnetic stirring. The final precipitates were filtered, washed with ethanol, and dried under a vacuum at room temperature for 24 h after the reaction keeping at room temperature for 30 min. A series of samples are prepared in solutions with different concentrations of starting materials (such as HF and $KMnO_4$). To investigate the influence of experimental procedure on the resulted products, three typical samples were prepared according to the synthetic parameters described in Table 1.

Table 1 The dependence of the color and luminescence intensity of the phosphors named KTFM (1–3) on the order of adding starting materials.

Order of addition	Step 1	Step 2	Step 3
KTFM-1	Solid+H_2O	$Ti(OR)_4$	HF
KTFM-2	Solid+H_2O	HF	$Ti(OR)_4$
KTFM-3	HF	$Ti(OR)_4$	Solid+H_2O

Note: Solid+H_2O denotes mixed starting materials 0.079 g $KMnO_4$, 1.16 g KF, and 20 mL H_2O; $Ti(OR)_4$ denotes starting material 3.5 mL $Ti(OC_4H_9)_4$ solution. HF denotes starting material 15 mL 40 wt. % HF solution.

The experimental process is schematically illustrated in Fig 1. For a typical preparation of KTFM-3, 3.5 mL $Ti(OR)_4$ was dropped into 15 mL 40 wt. % HF solution under magnetic stirring in a Teflon beaker and a translucent solution was formed. Subsequently, a purple solution including 0.079 g $KMnO_4$, 1.16 g KF, and 20

mL H_2O was dropped into the above solution. A precipitate was formed after the reaction mixture was kept at room temperature for 30 min. In some cases, TiO_2 was used as a titanium source for comparison. $Ti(OC_4H_9)_4$ was the titanium source in all reactions unless otherwise specified.

2.2. Characterization

The XRD measurements of the as-prepared samples were carried out on a D8 Advance (Bruker, Germany) x-ray powder diffraction using graphite monochromatized Cu Kα radiation (λ = 0.15406 nm). Phase identification was made using standard JCPDs files. The morphology and structure of the samples were studied by a field emission scanning electron microscopy (FE-SEM) on Nova NanoSEM 200 scanning electron microscope (FEI Inc.) with an attached energy dispersive spectrum (EDS). The amounts of Mn elements in precursor solution and filtrate were analyzed by Perkin Elmer Optima 8000 inductively coupled plasma–atomic emission spectroscopy (ICP-AES). UV-vis diffuse reflectance spectra were recorded on a Shimadzu UV-1800 spectrometer with a resolution of 1.0 nm. Photoluminescence (PL) spectra were recorded on FluoroMax-4 spectrofluorometer (Horiba Jobin Yvon Inc.) with a 150 W xenon lamp at room temperature. All excitation and emission spectra were measured at room temperature with identical instrumental parameters.

3. Results and discussion

3.1 Formation mechanism for red phosphor KTFM

The color and luminescence properties of the prepared phosphors are strongly

dependent on the order in which the starting materials are added. This indicates that the reactions by which the red phosphor KTFM forms are kinetically controlled. As shown in Fig. 1 and Fig. S1a,b†, sample KTFM-1 is a pale yellow powder and shows very weak red luminescence under UV light excitation. During KTFM-1 formation, $Ti(OC_4H_9)_4$ hydrolyzed to colloidal $Ti(OH)_4$ in neutral or alkaline solution as expressed by the following equation:

$$Ti(OC_4H_9)_4 + 4H_2O = 4C_4H_9OH + Ti(OH)_4 \quad (1)$$

At the same time, a redox reaction took place between $KMnO_4$ and $Ti(OC_4H_9)_4$ in the absence of HF:

$$4KMnO_4 + 3Ti(OC_4H_9)_4 + 8H_2O = 12C_4H_9O + 4MnO_2 + 4KOH + 3Ti(OH)_4 \quad (2)$$

As in previous work, traces of MnO_2 on the nanometer scale were not detectable in XRD of micro K_2SiF_6 crystals.[23]

With the addition of HF, the formation of KTF took place as follows:

$$Ti(OH)_4 + 2KF + 4HF = K_2TiF_6 + 4H_2O \quad (3)$$

MnO_2 cannot convert to $[MnF_6]^{2-}$ even in the presence of HF. The following reaction might take place instead:

$$2MnO_2 + 4HF = 2MnF_2 + O_2 + 2H_2O. \quad (4)$$

MnF_2 is soluble and remained in the filtrate. Here, pure phase KTF was obtained, but it showed very weak red luminescence in KTFM-1. KTFM-2 is white powder and showed red luminescence under UV light (Fig. S1c, d†). KTFM-3 is a pale orange powder and showed brighter red luminescence under UV light than KTFM-2 (Fig. S1e, f†). For KTFM-2 and KTFM-3, K_2MnF_6 formed as follows:

$$4KMnO_4 + 4KF + 20HF = 4K_2MnF_6 + 10H_2O + 3O_2 \quad (5)$$

The hydrolysis of $Ti(OR)_4$ was inhibited in the presence of HF. KTF can form in F^--rich solutions as follows:

$$Ti(OC_4H_9)_4 + 2KF + 4HF = K_2TiF_6 + 4C_4H_9OH \quad (6)$$

The simultaneous reactions of (5) and (6) yielded red phosphor KTFM. The XRD patterns of the typical three samples as indicated by the synthetic technique are given in Table 1 and Fig 2. All experimental parameters and conditions were identical for the three except for the order of starting materials addition. The reflection pattern of the three samples is consistent with the Joint Committee on Powder Diffraction Standards card data (JCPDs car no. 08-0488) of KTF with a hexagonal structure in a $P\bar{3}m1$ space group. Thus, the host lattice of hexagonal KTF can be readily obtained regardless of the experimental procedures. $KMnO_4$ decomposed to Mn (VII) and O_2 gas. The presence of HF is essential to the formation of K_2MnF_6 and makes it possible for the red phosphor KTFM to form. A small volume of HF solution is necessary for the cation exchange reaction between KTF and K_2MnF_6 in previous work.[25] The specific multiple functions of HF in this synthetic strategy might be attributable to the weakly acidic and complexing properties of HF. In the synthetic technique, HF serves as a weak acid that inhibits the hydrolysis of $Ti(OC_4H_9)_4$. It is also a complex and a fluridizer to form groups $[TiF_6]^{2-}$ and $[MnF_6]^{2-}$. reduces

Pure phases of hexagonal KTF can also be obtained by substituting $Ti(OC_4H_9)_4$ with TiO_2 as the titanium source as shown in Fig. S2a†. The reaction responsible for formation of KTF may be the following:

$$TiO_2 + 2KF + 4HF = K_2TiF_6 + 2H_2O \quad (7)$$

3.2 Morphology and determination of composition

Fig. 3 shows the morphology and composition of KTF and KTFM prepared by etching $Ti(OC_4H_9)_4$ in HF at room temperature. As visible in the SEM images, both KTF and KTFM had irregular morphologies with smooth surfaces, indicating strong crystallization. The diameters of the particles varied from 10 to 30 μm. Only the peaks of F, Ti, and K were detectable in the EDS of undoped KTF (Fig. 3b) . The molar ratio of F:Ti:K was about 6:1:2 indicating stoichiometric KTF. Elemental Mn was indentified in the EDS of red KTFM (Fig. 3d) and its atomic concentration is less than 0.5 %. The composition of red phosphor was further analyzed by X-ray photoelectron spectroscopy (XPS). Typical XPS survey scans of KTFM over a large energy range is presented in Fig. S2a†. It can be seen that it is mainly composed of elements K, Ti and F. The peak at 284.6 eV is ascribed to the contamination of CO_2 in air and carbon on the substrate. The signals of Mn^{4+} are very weak but can be observed in magnified spectrum of Mn^{4+} in Fig. S2a† insert. The two peaks at 642.5 eV and 654.2 eV are attributed to the binding energy of Mn element that confirms the presence of Mn^{4+} in the phosphor (Fig. S2a† insert). The low intensity of the photoelectron of Mn is consistent with the relatively low doping concentration. The atomic concentration of Mn^{4+} in the phosphor is about 0.16 mol % of Ti^{4+}. For comparison, KTFM was prepared by etching TiO_2 at room temperature. It was characterized by XRD, SEM and EDS in Fig. S2b-e†. XRD (Fig. S2b†) shows the pattern matches the standard pattern of pure KTF phase (JCPDs car no. 08-0488) with a hexagonal structure. SEM

images (Fig. S2c,d†) show that the particles are tetrahedrons with solid centers in the micrometer region, which are similar to those reported in a previous work.[24] The EDS in Fig. S2e† exhibits signals of elements F, Ti, K, and Mn in the as-prepared sample. The amount of Mn^{4+} in red KTFM prepared from TiO_2 is also lower than 1 mol% of Ti^{4+}. However, Mn^{4+} doping in KTF host lattice can still be confirmed by luminescence spectrum (Fig. S4†). MnO_2 often forms in $KMnO_4$-rich solutions (including 3 g $KMnO_4$ per 100 mL total volume).[23] This has not detected in the as-prepared samples.

3.3 Influence of experimental procedures, starting materials, and the concentration of $KMnO_4$ in precursor solutions.

The light absorption capability of KTF and KTFM have been evaluated using the reflectance from $BaSO_4$ as a reference. The undoped KTF powder was white and its reflectance reached 97% in the visible region as shown in Fig. 4a. In Fig. S3†, we see regular octahedrons of $[TiF_6]^{2-}$ in the hexagonal structure of KTF.[31] The activator Mn^{4+} ions occupy the Ti^{4+} sites randomly in the KTF host because they have the similar ionic radius and the same charge. The Mn^{4+}-doped KTF exhibits a strong and broadband absorption in the range of blue (Fig. 4b). This makes it possible to use the red phosphor KTFM on GaN-based white LEDs.

The luminescence intensity of the red phosphor was found to be strongly dependent on experimental procedure, starting materials, and the concentration of $KMnO_4$. Fig. 5 shows the emission spectra of phosphors KTFM-1, KTFM-2, and KTFM-3 excited at 467 nm. The spectra are very similar to those of Mn^{4+} doped complex fluorides

reported previously.[15-29] The three emission spectra were identical in shape and mainly composed of two parts. A group of emission peaks a below 620 nm was observed. These are most likely due to the anti-Stokes vibronic side bands associated with the excited state ^2E_g of Mn^{4+}. It disappeared at 78 K in $CaAl_{12}O_{19}:Mn^{4+}$ and $BaSiF_6:Mn^{4+}$.[12,29] The other group of peaks above 620 nm was attributed to the spin-forbidden ^2E_g-$^4A_2$ transition.[12-29] The zero-photon lines of ^2E_g-$^4A_2$ transition of Mn^{4+} cannot be detected at room temperature in our work, which was observed at a temperature below 30 K.[25] The luminescence of KTFM-1 was much weaker than KTFM-2 and KTFM-3 because reaction (2) rather than reaction (5) was dominant when HF was added in the last step. The primary difference between KTFM-2 and KTFM-3 in these experiments might be due to the difference in HF concentrations at the beginning of the reaction (5). Accordingly, the reactions by which red phosphor KTFM form were kinetically dominated. This was confirmed by change in the color of powders from white to pale orange. The influence of HF concentration on the properties of products will be discussed later. The red phosphor KTFM prepared from $Ti(OC_4H_9)_4$ showed a much higher luminescence intensity than that from TiO_2 (Fig. S4†). This might be because liquid $Ti(OC_4H_9)_4$ diffuses more readily than solid TiO_2, which make the mixture of starting materials a larger interface and the reaction more efficient at room temperature.

To determine the optimal doping concentration and to prevent the formation of MnO_2 contamination, a series of samples were prepared at different $KMnO_4$ concentrations (in precursor solution). This was because $KMnO_4$-rich precursor

solution could cause the formation of MnO_2. As shown in Fig. S5†, XRD patterns of all the samples prepared at different $KMnO_4$ concentrations were well indexed to the standard card data (JCPDs car no. 08-0488). There is no evident shift in reflections for the phosphor samples that is attributable to the very low concentrations of dopant Mn^{4+} in all the samples. Undoped KTF showed no absorption (Fig. 4a) or luminescence (Fig. 6a) in the visible region. We observed that the color of the powders changed from white to pale orange when the $KMnO_4$ concentration increased from 5 to 25 mmol.L^{-1}. The concentration of $KMnO_4$ had a pronounced effect on the luminescence intensities of the KTFM (Fig. 6a). The luminescence intensity increased as the concentration of $KMnO_4$ increased from 5 to 25 mmol.L^{-1}. The sample with highest luminescence intensity was obtained in the precursor solution with a $KMnO_4$ concentration of 25 mmol.L^{-1}. This was much lower than the 330 mmol.L^{-1} used in the previous work.[24]

To determine how much $[MnO_4]^-$ changes to $[TiF_6]^{2-}$, we carried out ICP-AES analysis on Mn elements in the filtrate (the solution after filtration), which includes Mn elements in various charge states, such as Mn (II) in Mn^{2+}, Mn (IV) in $[MnF_6]^{2-}$, and Mn (VII) in $[MnO_4]^-$. There were 32.4 mol% (0.1221 mmol) of Mn entered crystals and 67.6 mol% (0.3779 mmol) left in filtrate for the sample prepared in precursor solution enclosed of 25 mmol.L^{-1} $KMnO_4$. The doping concentration of Mn^{4+} in the solid state phosphor sample was about 0.12 mol% of Ti^{4+} based on the hypothesis that all $Ti(OC_4H_9)_4$ changes to $[TiF_6]^{2-}$ (about 1.0240 mol) completely. The solubility of KTF was about 0.17 g.mL^{-1} in 49 wt. % HF solution at room

temperature.[25] Thus, the actually optimal doping concentration of Mn^{4+} was a little higher than 0.12 mol% of Ti^{4+}, which approximates 0.16 mol% measured by XPS (Fig. S2a†). The results show that the optimum concentration of Mn^{4+} in red phosphor KTFM is much lower than those in conventional phosphors activated by rare earth ions.[32-34] The dominant $KMnO_4$ doses not enter host lattices as form of Mn^{4+} but is remained in the filtrate mainly as form of Mn^{2+}. When the concentration of $KMnO_4$ was larger than 25 $mmol.L^{-1}$, the pale orange color of powder became deeper and the luminescence intensity decreased. This was partly due to concentration quenching among Mn^{4+} ions. More importantly, samples prepared from $KMnO_4$-rich solution may have been contaminated with MnO_2,[23] which cannot be detected by XRD because the diffraction peaks of nanosized MnO_2 are much wider and lower than those of complex fluorides on the μm scale. Correspondingly, the decay times of 631 nm emissions (excited at 467 nm) of all the samples prepared from precursor with different $KMnO_4$ concentrations has been measured at room temperature (Fig. S6†). All the decay curves fit a single exponential well. The decay time decreased as $KMnO_4$ concentration increased; this was indicative of increasing exchange interaction probability between Mn^{4+} pairs.

3.4 Influence of HF concentration on structure, luminescence, and yield

Fig. 7 shows XRD patterns of red phosphors KTFM prepared at different HF concentrations. It should be noted that a phase KTF with a structure that matches the standard card JCPDs closely (#28-0825) was detected at HF concentration of 5 wt. %,. This is the first observation of red luminescence of Mn^{4+} doped KTF with this

structure. The structure transformation emerged with increasing HF concentration. The phases were found to be hexagonal structured KTF when HF concentrations were 10 wt. % or higher, as can be determined by the positions and intensity of peaks shown in Fig. 7b–e.

The effects of HF concentration on the luminescence of KTFM are shown in Fig. S7† (excitation spectra) and Fig. 8 (emission spectra). As shown in Fig. S7†, the excitation spectra showed three absorption bands from 200 to 520 nm with a maximum absorption band in blue. The weak excitation band at 240-300 nm is originated from charge transfer transition of F^--Mn^{4+}.[25] The broad excitation band at 320-400 nm is attributed to the spin and parity forbidden transition $^4A_2$-$^4T_1$ transitions of Mn^{4+}. The strongest absorption band locating in blue region at 400-510 nm is originated from $^4A_2$-$^4T_2$ transitions of Mn^{4+}. Its full width at half emission maximum (FWHM) is about 50 nm that matches well the dominant GaN based LEDs (with electroluminescence wavelength at 460 nm and FWHM of 20 nm). The phosphor KTFM has little absorption in green/yellow (530-590 nm) region but the excitation spectra of commercialized red phosphor $M_2Si_5N_8:Eu^{2+}$ (M=Ca, Sr and Ba) are extended from near UV to orange region.[35] Therefore, lower re-absorption of red phosphor KTFM would lead to higher luminescence conversion efficiency than $M_2Si_5N_8:Eu^{2+}$ when they are fabricated with yellow phosphor YAG:Ce on GaN chips to compensate red component in the spectra. The sample of KTFM prepared at 5 wt. % HF showed the lowest luminescence intensity. The color of the as-prepared powders changed from white to light yellow and pale orange as the HF concentration

increased. This indicated that high HF concentrations might help form high concentrations of Mn^{4+} dopants.

We assumed that the dependence of luminescence intensities on HF concentration was attributable to variations in Mn^{4+} concentrations in crystals. As shown in Fig. S8†, the tendency of decay times changing with HF concentration confirmed this hypothesis. The decay time of 631 nm emissions of red phosphor K_2TiF_6:Mn^{4+} (excited at 467 nm) decreases with HF concentration increasing, which shows higher exchange interaction between neighboring Mn^{4+} pairs for the samples obtained at a solution with higher HF concentration. The yield was in inversely proportional to the concentration of HF as shown in Fig. 9a. This should be attributed to the fact that KTF can dissolve in HF with a high enough concentration. No solid product can be obtained in 50 wt. % HF solution in our experiment. The luminescence intensity increases linearly with HF concentration as shown in Fig. 9b. The optimized luminescence intensity was determined for the solution with HF concentration at 40 wt. % The increased luminescence intensity obtained by increasing HF concentration might be due to higher molar ration of $[MnF_6]^{2-}$ entering the host lattice. This can also explain why the luminescence intensity of sample KTFM-3 was higher than that of KTFM-2.

3.5 Thermal stability of phosphor KTFM

The thermal stability of K_2TiF_6:Mn^{4+} has not been investigated in previous reported works so far. However, it was observed that the decomposition of the similar compound Na_2TiF_6 below 1073 K was insignificant and it decomposed to 50% at

1273 K.[36,37] The thermal stability of phosphor KTFM was investigated by thermogravimetrics (TG) and different scanning calorimeter (DSC) as shown in Fig. S9†. An endothermic peak at 380.2 ^{o}C is due to the release of loosely bound water on the surfaces of crystals. The weight of the sample remains almost unchanged up to 737.2 ^{o}C. The KTFM begins to decompose above 737.2 ^{o}C. The TG and DSC characters of KTFM are quite different from those of K_2SiF_6:Mn^{4+} and Ba_2TiF_6:Mn^{4+}.[23,26] The decomposition temperatures of K_2SiF_6:Mn and Ba_2TiF_6:Mn are 362 ^{o}C and 400 ^{o}C, respectively. Therefore, the prepared red phosphor KTFM is thermally stable and can be used in white LED lightning.

3.6 Application of KTFM in LEDs

The superior thermal stability of KTFM make it a potential candidates for application in high-power LEDs. As shown in Fig. S10†, a LED fabricated with KTFM on GaN chip shows perfect purple light that is hard to realize through mixing conventional blue and red phosphors with excitation at UV region due to re-absorptions. A "warm" white LED is fabricated with the as-prepared red phosphor KTFM and YAG:Ce^{3+} on GaN chip. The white light driven at 20 mA has a color rendering of 86 at 3251 K.

4. Conclusion

In conclusion, red phosphors KTFM with improved luminescence intensities have been synthesized by etching $Ti(OC_4H_9)_4$ in HF with $KMnO_4$ and KF at room temperature. In these cases, HF is a key factor for the formation of luminescence

centers of Mn^{4+} in the KTF host lattice. The concentration of $KMnO_4$ in precursor solution varied from 0 to 60 mmol.L^{-1} and the optimal concentration was 25 mmol.L^{-1}. This was much lower than the 330 mmol.L^{-1} used in previous work.[24] ICP-AES analysis of the concentration of Mn in the filtrate indicated that the optimal Mn^{4+} concentration doped into KTF crystals was about 0.12 mol% of Ti^{4+} which approximates that measured by XPS . The red luminescence of Mn^{4+} doped in KTF matched the standard card JCPDs (#28-0825) was firstly observed. The pale orange color of the as-prepared powders became deeper as the HF concentration increased, indicating that high HF concentration might facilitate the formation of high concentrations of Mn^{4+} dopants because that is helpful to forming group $[MnF_6]^{2-}$. However, no solid state product can be obtained when HF concentration arrived at 50 wt. %, which is due to the solubility of KTF in high concentrated HF solution. KTF took on a hexagonal structure and the yield of red phosphor decreased as HF increased in concentration from 5 to 40 wt. %. The remarkably high rendering of white LEDs was attributed to the compensation of red components by fabricating as-prepared red phosphor KTFM with commercially available yellow phosphor YAG:Ce.

Acknowledgments

This research was jointly supported by Chinese NSF (Grant no.51102185) and Qianjiang Talents Project (Grant no. QJD1302005).

References

1 J. J. Wierer, J. Y. Tsao and D. S. Sizov, *Laser Photon. Rev*., 2013, **7**, 963.

2 C. J. Humphreys, *MRS Bull.*, 2008, **33**, 459.

3 R. J. Xie and N. Hirosaki, *III-Nitride Based Light Emitting Diodes and Applications, Topics in Appl. Phys.*, Springer., 2013, **126**, 291.

4 A. A. Setlur, W. J. Heward, Y. Gao, A. M. Srivastava, R. G. Chandran and M. V. Shankar, *Chem. Mater.*, 2006, **18**, 3314.

5 T. S. Chan, R. S. Liu and I. Baginskiy, *Chem. Mater.*, 2008, **20**, 1215.

6 H. Chen, Method for manufacturing a triple wavelengths white LED，*U.S. Patent* 20100040769 A1, Feb. 18, 2012.

7 X. D. Li, J. G. Li, Z. M. Xiu, D. Huo and X. D. Sun, *J. Am. Ceram. Soc.,* 2010, **93**, 2229.

8 W. Cheng and C. Lien, Method of enhancing color rendering index of a white LED，*U.S. Patent* 20130143334 A1, Jun. 6, **2013**.

9 K. A. Denault, A. A. Mikhailovsky, S. Brinkley, S. P. DenBaarsab and R. Seshadri, *J. Mater. Chem*. C, 2013, **1**, 1461.

10 S. E. Brinkley, N. Pfaff, K. A. Denault, Z. Zhang, H. T. (Bert) Hintzen, R. Seshadri, S. Nakamura and S. P. DenBaars, *Appl. Phys. Lett*., 2011, **99**, 241106.

11 H. Brunner, T. Fiedler, F. Jermann, J. Strauβ, M. Zachau, White-emitting LED having a defined color temperature. *U.S. Patent* 7965031 B2, Jun. 21, **2011**.

12 Y. X. Pan and G. K. Liu, *J. Lumin.*, 2011, **131**, 465.

13 T. Takahashi and S. Adachi, *Electrochem. Solid-State Lett*., 2009, **128**, J69.

14 C. Liao, R. Cao, Z. Ma, Y. Li, G. Dong, K. N. Sharafudeen and J. R. Qiu, *J. Am.*

Ceram. Soc., 2013, **96**, 3552.

15 S. Adachi and T. Takahashi, *J. Appl. Phys.*, 2008, **104**, 023512.

16 R. Kasa and S. Adachi, *J. Appl. Phys.*, 2012, **112**, 013506.

17 S. Adachi and T. Takahashi, *J. Appl. Phys.*, 2009, **106**, 013516.

18 N. Mega and O. Kazuyoshi, *Jpn. J. Appl. Phys.*, 2012, **51**, 022604.

19 T. Takahashi and S. Adachi, *Electrochem. Solid-State Lett.*, 2009, **12**, J69.

20 T. Takahashi and S. Adachi, *J. Electrochem. Soc*., 2008, **155**, E183.

21Y. K. Xu and S. Adachi, *J. Appl. Phys*., 2009, **105**, 013525.

22 T. Takahashi and S. Adachi, *Electrochem. Solid-State Lett*., 2009, **128**, J69.

23 L. F. Lv, X. Y. Jiang, S. M. Huang, X. A. Chen, Y. X. Pan, *J. Mater. Chem. C*, 2014, **2**, 3879.

24 Y. K. Xu and S. Adachi, *J. Electrochem. Soc*., 2011, **158**, J58.

25 H. M. Zhu, C. C. Lin, W. Q. Luo, S. T. Shu, Z. G. Liu, Y. S. Liu, J. T. Kong, E. Ma, Y. G. Cao, R. S. Liu and X. Y. Chen, *Nat. Commun.*, 2014, **5**, 4312..

26 X. Y. Jiang, Z. Chen, S. M. Huang, J. G. Wang, Y. X. Pan, Dalton Trans. 43, 2014, 9414-9418. *Dalton Trans.*, 2014, **43**, 9414.

27 D. Sekiguchi and S. Adachi, *ECS J. Solid State Sci. Tech.*, 2014, **3**, R60.

28 D. Sekiguchi, J. Nara and S. Adachi, *J. Appl. Phys.*, 2013, **113**, 183516.

29 X. Y. Jiang, Y. X. Pan, S. M. Huang, X. A. Chen, J. G. Wang and G. K. Liu, *J. Mater. Chem. C*, 2014, **2**, 2301.

30 H. W. Roesky, *Efficient Preparations of Fluorine Compounds*, Hoboken, N.J Wiley, 2013.

31 O. Gobel, *Acta Crystallogr. C* 2000, **56**, 521.

32 C. Y. Xu, Y. D. Li, Y. L. Huang, Y. M. Yu and H. J. Seo, *J. Mater. Chem. C*, 2012, **22**, 5419.

33 J. Y. Han, W. B. Im, G. Y. Lee and D. Y. Jeon, *J. Mater. Chem. C*, 2012, **22**, 8793.

34 D. L. Geng, G. G. Li, M. M. Shang, D. M. Yang, Y. Zhang, Z. Y. Cheng and J. Lin, *J. Mater. Chem. C*, 2012, **22**, 23789.

35 R. Mueller-Mach, G. O. Mueller, M. R. Krames, H. A. Höppe, F. Stadler, W. Schnick, T. Juestel and P. Schmidt, *Phys. Status Solidi A*, 2005, **202**,1727.

36 V. A. Reznichenko, V. P. Solomakha, and A. A. Poroskov, Deposited Publ,, 1972, VINITI 5864 (*Chem. Abs.*, 1976, **85**, 13235).

37 B. F. G. Johnson, *Inorganic Chemistry of the Transition Elements:* Volume **6** (Specialist Periodical Reports), (Volume **6** of the Proceedings, Butterworths, 1971).

Figure caption：

Fig. 1. Schematic of synthesis effects on luminescence intensity of the phosphor samples KTFM-1, KTFM-2, and KTFM-3 prepared according to the detailed experimental process in Table 1.

Fig. 2. XRD patterns of samples (a) KTFM-1, (b) KTFM-2, and (c) KTFM-3 prepared according to the detailed experimental process in Table 1.

Fig. 3. SEM images and EDS spectra of (a) K_2TiF_6 and (b) K_2TiF_6:Mn^{4+} prepared by etching $Ti(OC_4H_9)_4$ in HF at room temperature.

Fig. 4. Diffuse reflection spectra of (a) undoped K_2TiF_6 and (b) red phosphor K_2TiF_6:Mn^{4+} (named KTFM-3) prepared in our experiments.

Fig. 5. Emission spectra of samples (a) KTFM-1, (b) KTFM-2, and (c) KTFM-3 excited at 467 nm.

Fig. 6. Emission spectra (excited at 467 nm) of red phosphor K_2TiF_6 :Mn^{4+} prepared by wet chemical etching at room temperature with $KMnO_4$ concentration at (a) 0, (b) 5, (c) 10, (d) 25, (e) 30, and (f) 60 $mmol.L^{-1}$.

Fig. 7. XRD patterns of red phosphors K_2TiF_6 :Mn^{4+} prepared by wet chemical etching at room temperature with HF concentration at (a) 5, (b) 10, (c) 20, (d) 30, and (e) 40 wt. %.

Fig. 8. Emission spectra of red phosphors K_2TiF_6 :Mn^{4+} prepared by wet chemical

etching at room temperature with HF concentration of (a) 5, (b) 10, (c) 20, (d) 30, and (e) 40 wt. %.

Fig. 9. Dependence of (a) sample yield and (b) luminescence intensity on concentration of HF.

Figures:

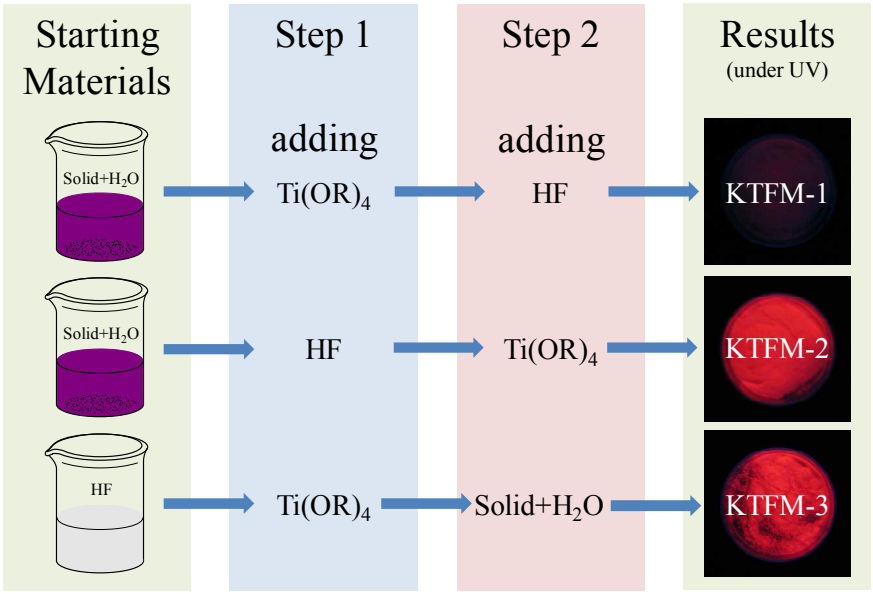

Fig. 1

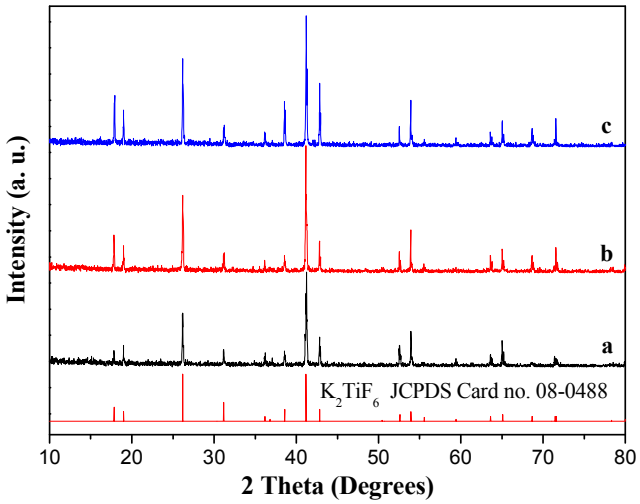

Fig. 2

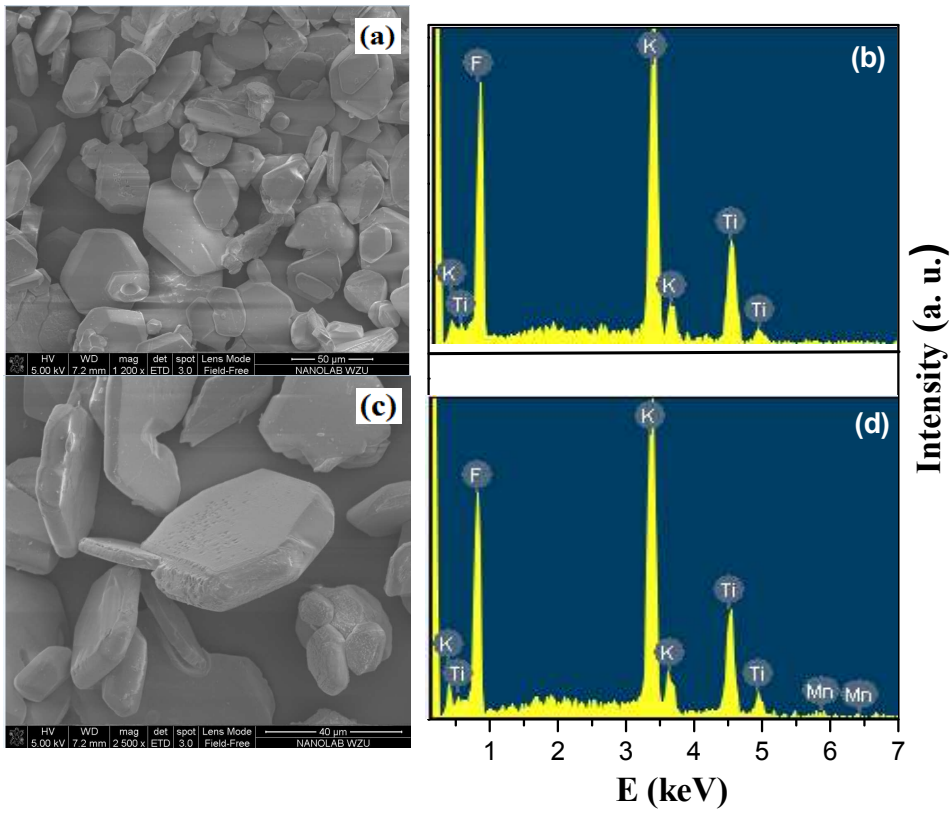

Fig. 3

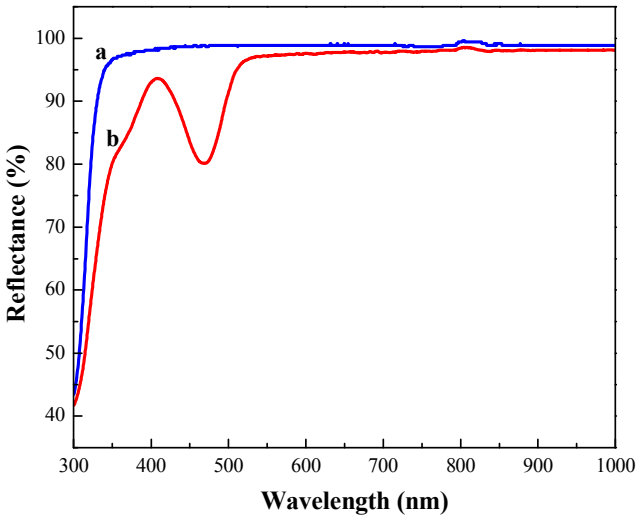

Fig. 4

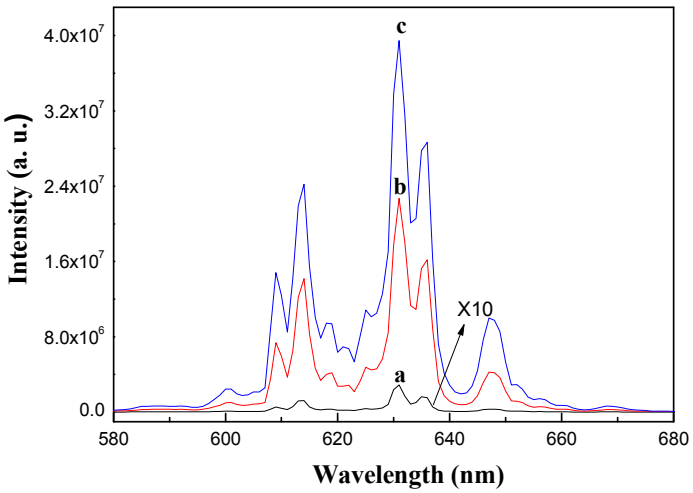

Fig. 5

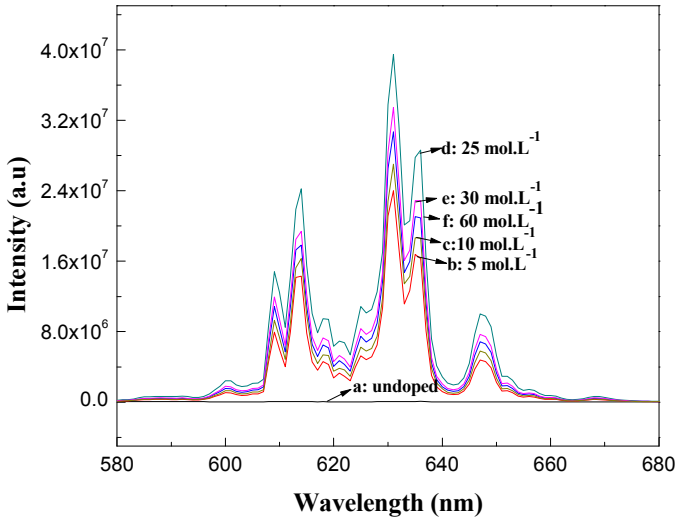

Fig. 6

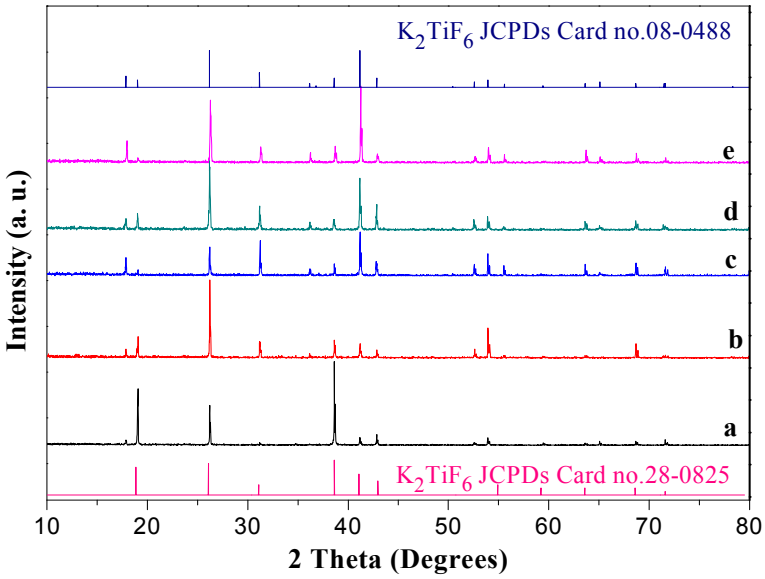

Fig. 7

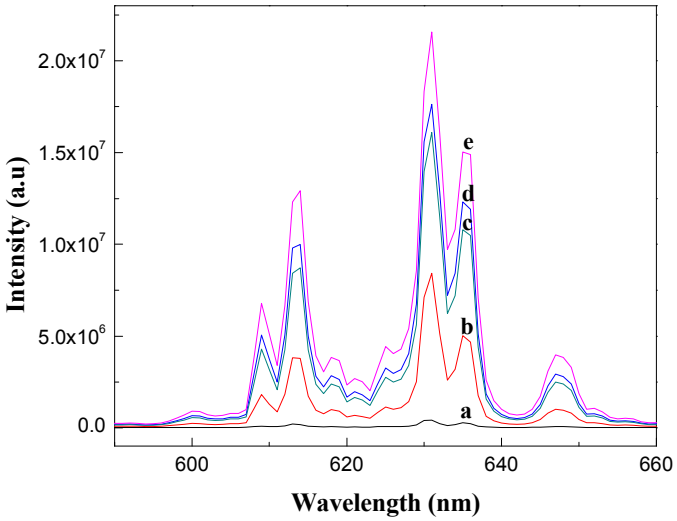

Fig. 8

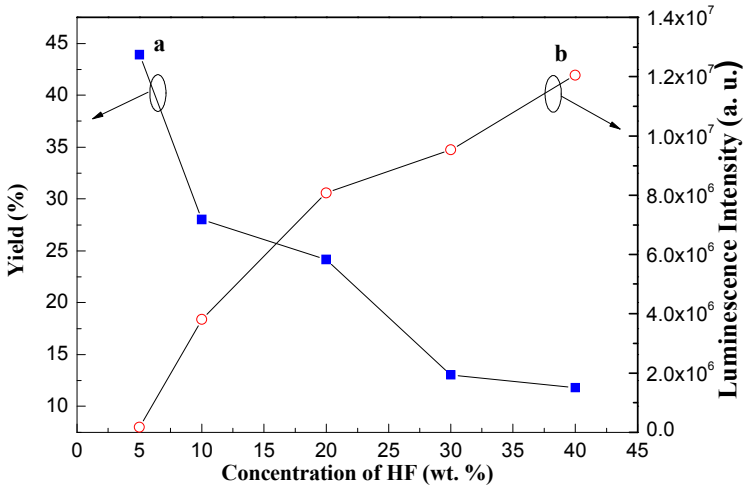

Fig. 9

Graphical Abstract

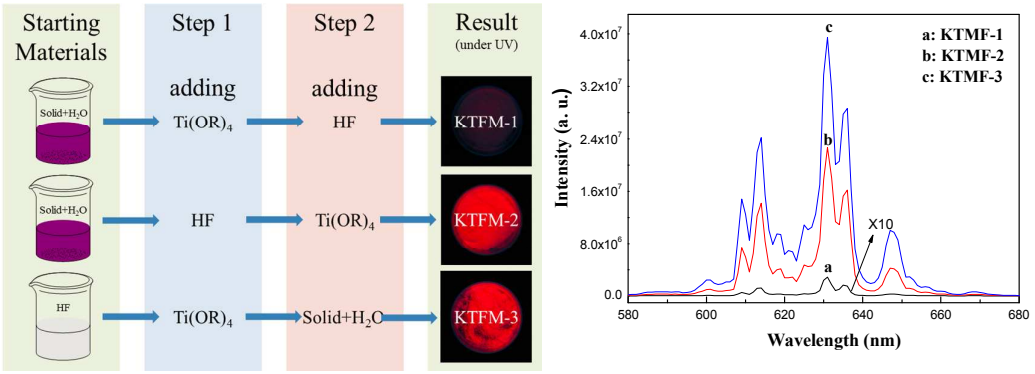

The formation mechanism for red phosphors $K_2TiF_6:Mn^{4+}$ synthesized by etching $Ti(OC_4H_9)_4$ in HF at room temperature has been discussed. The luminescence intensity has been improved by optimizing synthetic process and the concentrations of HF and/or $KMnO_4$. Encapsulation of the red phosphor $K_2TiF_6:Mn^{4+}$ with YAG:Ce on a GaN layer produces "warm" white LEDs with high color rendering 86 at 3251 K.